Published in final edited form as:
Biomaterials. 2012 September ; 33(26): 6123–6131. doi:10.1016/j.biomaterials.2012.05.027.

Spatial Control of Cell-Mediated Degradation to Regulate Vasculogenesis and Angiogenesis in Hyaluronan Hydrogels

Donny Hanjaya-Putra[1], **Kyle T. Wong**[1,2], **Kelsey Hirotsu**[1], **Sudhir Khetan**[3], **Jason A. Burdick**[3], and **Sharon Gerecht**[1,§]

[1]Department of Chemical and Biomolecular Engineering, Johns Hopkins Physical Sciences-Oncology Center and the Institute for NanoBioTechnology, The Johns Hopkins University, 3400 N. Charles St., Baltimore, Maryland 21218, USA

[2]Department of Biomedical Engineering, The Johns Hopkins University, 3400 N. Charles St., Baltimore, Maryland 21218, USA

[3]Department of Bioengineering, University of Pennsylvania, Philadelphia, PA 19104 USA

Abstract

Matrix remodeling is crucial for neovascularization, however its utilization to control this process in synthetic biomaterials has been limited. Here, we utilized hyaluronic acid (HA) hydrogels to spatially control cellular remodeling during vascular network formation. Specifically, we exploited a secondary radical polymerization to alter the ability of cells to degrade the hydrogel and utilized it to create spatial patterning using light initiation. We first demonstrated the ability of the hydrogel to either support or inhibit *in vitro* vasculogenesis of endothelial colony-forming cells (ECFCs) or angiogenesis from *ex ovo* chorioallantoic membranes. We showed that vascular tube branching and sprouting, which required matrix metalloproteinases (MMPs)-dependent remodeling, could be achieved in hydrogels formed by primary addition-crosslinking only. Although ECFCs expressed higher levels of MMPs in the hydrogels with the secondary radical-crosslinking, the generated kinetic chains disabled cell-mediated remodeling and therefore vascular formation was arrested at the vacuole and lumen stage. We then patterned hydrogels to have regions that either permitted or inhibited cell-mediated degradation during *in vitro* vasculogenesis or angiogenesis. Our ability to control degradation cues that regulate vascular tube formation is important for the study of vascular biology and the application of synthetic biomaterials in tissue regeneration.

Keywords

Hyaluronic Acid/Hyaluronan; Hydrogels; Endothelial Colony-Forming Cells; Angiogenesis; Vasculogenesis; Spatial Control

1. Introduction

The vascular system is formed through both vasculogenesis, the *de novo* formation of blood vessels, and angiogenesis, the sprouting of vessels from a preexisting vascular tube [1, 2].

§To whom correspondence should be addressed. Tel: 410-516-2846, Fax: 410-516-5510, gerecht@jhu.edu.

Bone marrow-derived endothelial colony-forming cells (ECFCs) participate in vascular repair and regeneration through postnatal vasculogenesis and angiogenesis [3]. In response to stimuli, ECFCs migrate, differentiate, degrade the extracellular matrix (ECM), and undergo tubulogenesis. These processes are spatiotemporally regulated by biochemical and biophysical cues of the ECM [4]. Much of our understanding of these molecular regulations has been elucidated by the development of well-defined *in vitro* vasculogenesis and angiogenesis models using natural ECM, such as matrigel, collagen, and fibrin gels [5–8]. Many angiogenic factors have been identified to stimulate and "permit" angiogenesis [9, 10], while other small molecules have been found to "inhibit" angiogenesis and have been developed as drugs to inhibit tumor growth [11]. In addition, different ECM components have also been shown to "permit" or "inhibit" angiogenesis [12, 13].

Spatial control over vascular formation is essential for the generation of well organized vascular networks toward application in tissue regeneration [2, 14–16]; however, such control is difficult to achieve in natural matrices due to their inherent chemical and physical properties, which limit their manipulability. Synthetic biomaterials have been suggested as a xeno-free and more clinically relevant alternative for therapeutic vascularization [17, 18] and vascular network formation [19, 20]. Due to their versatility, these synthetic biomaterials can be designed with the incorporation of biochemical cues, such as soluble factors, cell adhesion, and degradation sites to provide instructive microenvironments to recapitulate complex stages of vascular morphogenesis [21]. Furthermore, recent study exploited spatial control over cell adhesion to guide the formation of well-organized vasculatures in PEG-based hydrogels [22]. Here we sought to explore cell-mediated degradation to provide spatial control over vascular morphogenesis. Although ECM remodeling has been shown to occur during vasculogenesis and angiogenesis [23, 24], its utilization in controlling these processes in synthetic biomaterials has been limited [25]. Using our basic understanding of polymer chemistry and vascular cell-mediated degradation, we can manipulate synthetic biomaterials to provide controlled remodeling cues, which are either "permissive" or "inhibitory" to vascular tube formation.

Hyaluronic acid (HA; hyaluronan) plays an important role in vascular development by regulating cell proliferation and migration [26]. Using HA as the primary structural component, we have developed hydrogels with high water content that promote cell viability [27]. In a previous study, we engineered a modular culture environment using HA hydrogels to precisely regulate the signaling pathways of ECFC vascular morphogenesis and generate functional microvascular networks. We showed that RGD integrin-binding is required in a dose-dependent manner to initiate vacuole and lumen formation. We then demonstrated that further progression of vascular morphogenesis through branching and sprouting to form complex vascular networks relies on matrix-metalloproteinases (MMPs)-dependent mechanisms [28]. In this report, we extend our previous studies by the incorporation of sequential crosslinking methods to enable spatial control over vascular remodeling. This technique has been previously used to spatially control the spreading [29] and differentiation [30] of human mesenchymal stem cells (hMSCs). It exploits the reactivity of vinyl groups within the HA macromer to create regions that are "permissive" or "inhibitory" to cell-mediated degradation, including vascular remodeling by *ex ovo* chorioallantoic (CAM) vessels or ECFCs *in vitro*.

2. Materials and methods

2.1. Human ECFCs

Human umbilical cord blood ECFCs isolated from outgrowth clones, kindly provided by Dr. Merv C. Yoder, Indiana University School of Medicine, were expanded and used for experiments between passages 6 and 8, as previously described [31–33]. Briefly, ECFCs

were expanded in flasks coated with type I collagen (Roche Diagnostics, Basel, Switzerland), in endothelial growth medium (EGM; PromoCell Heidelberg, Germany) supplemented with 1 ng/ml $VEGF_{165}$ (Pierce, Rockford, IL), and incubated in a humidified incubator at 37°C in an atmosphere containing 5% CO_2. ECFCs were passaged every three to four days with 0.05% trypsin (Invitrogen, Carlsbad, CA) and characterized for their endothelial cell (EC) surface markers and proliferative potential.

2.2. Synthesis of AHA hydrogels

Acrylated HA (AHA) was prepared as previously reported [29]. Briefly, AHA was synthesized using a two-step protocol: (1) the tetrabutylammonium salt of HA (HA-TBA) was produced by reacting sodium hyaluronate (64 kDa; Lifecore Biomedical, Chaska, MN) with the highly acidic ion exchange resin Dowex-100 and neutralized with 0.2 M TBA-OH; (2) acrylic acid (2.5 Eq) was coupled to HA-TBA (1 Eq, repeat unit) in the presence of dimethylaminopyridine (DMAP; 0.075 Eq) and di-tert-butyl dicarbonate (1.5 Eq) in DMSO, followed by dialysis and lyophilization. ^{1}H NMR was used to assess the modification of HA with acrylate functional groups.

2.3. Peptides

From GenScript Corporation (Piscataway, NJ, USA), we obtained the cell adhesive peptide GCGYG***RGD***SPG (MW: 1025.1 Da; bold italics indicates the RGD integrin-binding domain), MMP-sensitive crosslinker GCRDGPQG↓IWGQDRCG (MW: 1754.0 Da; down arrow indicates the site of proteolytic cleavage), and MMP-insensitive crosslinker GCRDGDQGIAGFDRCG (MW: 1754.0 Da), all with > 95% purity (per manufacturer HPLC analysis).

2.4. In vitro vasculogenesis assay

The *in vitro* vascuologenesis was assessed in AHA hydrogels as previously reported [28]. Briefly, AHA (3 wt%) was dissolved in a sodium phosphate buffered saline (NaPBS buffer: 0.1 M sodium phosphate, 0.3 M total osmolarity, pH 8.0) containing Irgacure 2959 (I2959, Ciba) photoinitiator (final concentration of 0.05 wt%). The cell adhesive peptides (RGDS; GenScript) were dissolved in NaPBS buffer and added to the AHA solution at final peptide concentrations of 3.7 mM (corresponding to 10% of available acrylate groups within 3 wt% AHA) and were allowed to react for one hour with gentle shaking. Recombinant human $VEGF_{165}$ (Pierce, Rockford, IL), bFGF (Invitrogen, Carlsbad, CA), Ang-1 (R&D, Minneapolis, MN), tumor necrosis factor-alpha (TNF-α; R&D) and stromal cell-derived factor-1 (SDF-1; R&D) were added at 50 ng/ml into the AHA-RGDS mixture. Human umbilical cord blood ECFCs were encapsulated in HA hydrogels with densities of 5×10^6 cells/ml. Following the resuspension of cells into this solution, MMP peptide crosslinker (MMP, GenScript) dissolved in NaPBS buffer was added at 4.83 mM (corresponding to the 25% of available acrylate groups within 3 wt% AHA). Immediately after adding the MMP crosslinker, 30 μl of this mixture was pipetted into sterile molds (5 mm diameter, 2 mm height), and was allowed to react for 15 minutes at room temperature inside the laminar flow hood. The constructs were cultured for up to three days in EGM (PromoCell). Visualization and image acquisition were performed using an inverted light microscope (Olympus IX50, Center Valley, PA) and a confocal microscope (LSM 510 Meta, Carl Zeiss, Inc., Thornwood, NY) at various time intervals along the culture period.

2.5. In vitro angiogenesis assay

In vitro angiogenesis into the synthetic HA hydrogel was assessed based on a previously established method using collagen or fibrin gels [34]. Briefly, AHA hydrogels were made as described above with the addition of sphingosine-1-phosphate (S1P, Avanti Polar Lipis,

Alabaster, AL) at a concentration of 125 μM. Human umbilical cord blood ECFCs were seeded on top of the AHA hydrogels and cultured for up to 3 days to allow invasion into the gels. Visualization and image acquisition were performed using an inverted light microscope (Olympus IX50, Center Valley, PA) and a confocal microscope (LSM 510 Meta, Carl Zeiss, Inc., Thornwood, NY) at various time intervals during the culture period.

2.6. Spatial patterning of HA hydrogels with UV crosslinking

To spatially pattern the AHA hydrogels, UV light was used to crosslink the free available acrylate groups as previously reported [30]. Stable AHA hydrogels, as described above [28], were termed uniform "−UV" hydrogels and used as a control, which was expected to support cell-mediated degradation. Selected "−UV" hydrogels were then exposed to 10 mW/cm^2 365 nm ultraviolet light (Omnicure S1000 UV Spot Cure System, Exfo, Ontario, Canada) for 2 minutes (secondary crosslinking) through glass coverslips to produce uniform "+UV" hydrogels. To obtain patterned AHA hydrogels, 10k DPI photomasks (CAD/Art Service, Inc., Bandon, OR) with stripes with specific widths as detailed in the text were used in the secondary crosslinking step. To visualize the "+UV" regions of the gels, 5 nM methacrylated rhodamine (MeRho) was mixed into the pre-polymer solution (methacrylate groups react extensively during the secondary radical polymerization, but compared to acrylate groups, crosslinking is too slow during the primary addition reaction) [29].

2.7. Ex ovo angiogenesis assay using CAM model

The CAM assay was prepared *ex ovo* as previously described [18, 25, 35]. Fertilized white leghorn chicken eggs (B&E Eggs Inc., York Springs, PA) were received at embryonic development day (EDD) 0 and incubated for 3 days at 37 °C in a constant humidified incubator with automatic turning (Hova Bator, GQF Manufacturing Company, Savannah, GA). On EDD 3, eggs were rinsed with betadine and 70% ethanol and opened into a 20 × 100 mm^2 petri dish (BD Falcon) under aseptic conditions. Then, 10 ml of DMEM-11965 (Invitrogen) containing 200 units/ml of gentamycin and myostatin were added onto the *ex ovo* culture. The dish was placed inside a larger 25 × 150 mm petri dish (BD Falcon) containing a thin layer of water for humidification, covered, and incubated at 37 °C in a humidified atmosphere of 2% CO_2. On EDD 8, + and −UV hydrogels were placed onto the CAM membrane and were cultured until EDD 12. The angiogenic response was evaluated by analyzing the convergence of blood vessels toward and inside the graft using a stereomicroscope (Unitron, Commack, NY). The graft and membrane constructs were then harvested, fixed with 3.7% formaldehyde (Sigma), and either stained with fluorescein-conjugated *Lens culinaris* lectin (1:40, Vector Lab) for confocal imaging (LSM 510 Meta, Carl Zeiss, Inc., Thornwood, NY) or processed for histological analysis.

2.8. Histological sectioning and staining

Following fixation of construct explants, samples were dehydrated in graded ethanol (70 to 100 percent), embedded in paraffin, serially sectioned using a microtome (5μm), and stained with hematoxylin and eosin (H&E). A minimum of six images were analyzed for each construct.

2.9. Viscoelasticity assessment

The oscillatory shear of the elastic modulus (G′) was measured using a constant strain rheometer with steel cone-plate geometry (25 mm in diameter; RFS3; TA Instruments, New Castle, DE), as previously described [31, 32, 36]. Briefly, we performed oscillatory time sweeps on three samples (n=3) for each hydrogel group at various time intervals along the culture period. The strain was maintained at 20% during the time sweeps by adjusting the stress amplitude at a frequency of 1 Hz. This strain and frequency were chosen because G′

was roughly frequency-independent within the linear viscoelastic regime. The tests occurred in a humidified chamber at a constant temperature (25 °C) in 30-second intervals. The You ng's modulus (substrate viscoelasticity) was calculated by $E = 2G'(1 + \nu)$. AHA hydrogels are assumed to be incompressible [31, 32, 37] such that their Poisson's ratios (ν) approach 0.5 and the relationship becomes $E = 3G'$ [36].

2.10. VEGF release and degradation study

At various time points, 1 mL of conditioned media from gels alone and from gels containing cells was collected and replaced with fresh growth media. At the final time point (day 3), the gels were degraded using endogenous 1,000 IU/ml hyaluronidase IV (Sigma, St. Louis, MO) for 24 hours. The samples of conditioned media were collected (n=3) and stored at −80 °C before being quantified for uronic acid (UA) and VEGF using ELISA kits (Pierce Biotechnology; Rockford, IL) following the manufacturer's instructions and as reported in our previous publications [28, 32, 38]. Results are presented in terms of cumulative release as a function of time.

2.11. Swelling ratio

The swelling ratio was gravimetrically measured as previously reported [39]. The pre-dried hydrogel specimens were immersed in distilled water at room temperature. The swollen hydrogels were removed from water at various time points and weighed after wiping off excess water from the surface with a filter paper. The swelling ratio was then calculated according to the following formula:

$$Swelling\ ratio = \frac{W_{s,t} - W_d}{W_d} \times 100\%$$

Where W_d is the weight of the dry hydrogels, and $W_{s,t}$ is the weight of the swollen hydrogels at time t. The hydrogels were assumed to reach a state of swelling equilibrium when there was no difference in the swelling ratio between two adjacent time intervals.

2.12. Real-time RT-PCR

Two-step RT-PCR was performed for *MT1-MMP, MMP-1, MMP-2, HPRT1* and *β-ACTIN*, and samples were examined in triplicate, analyzed, and graphed (n=3) as previously described [31, 32]. Briefly, total RNA was extracted using TRIzol (Gibco, Invitrogen Co., Carlsbad, CA) according to the manufacturer's instructions. Total RNA was quantified by an ultraviolet spectrophotometer, and the samples were validated for no DNA contamination. RNA (1 μg per sample) was reverse transcribed using M-MLV (Promega Co., Madison, WI) and oligo(dT) primers (Promega Co.) according to the manufacturer's instructions. TaqMan Universal PCR Master Mix and Gene Expression Assay (Applied Biosystems, Foster City, CA) for *MMP-1, MMP-2, MT1-MMP*, *HPRT1* and *β-ACTIN* were used according to manufacturer's instructions. The TaqMan PCR step was performed in triplicate with an Applied Biosystems StepOne Real-Time PCR system (Applied Biosystems). The relative expression of *MMP1, MMP2,* and *MT1-MMP* was normalized to the amount of *HPRT1 or β-ACTIN* in the same cDNA by using the standard curve method described by the manufacturer. For each primer set, the comparative CT method (Applied Biosystems) was used to calculate amplification differences between the different samples. The values for experiments (n=3) were averaged and graphed with standard deviations.

2.13. Zymography

The conditioned media from each culture conditions at various time points was collected and analyzed for MMP activity by SDS-PAGE under nonreducing conditions as previously described [25, 40]. Briefly, conditioned media from various time points was loaded on 10% Gelatin and 12% Casein zymography gels (Bio-Rad). Electrophoresis was carried out for 45 min at room temperature. After washing the gels in water, SDS was extracted from acrylamide gels with 2.5% Triton X-100 for 2 × 30 min. MMP activities were developed in a buffer, pH 8.0, containing 50 mM Tris-HCl, 5 mM CaCl2 and 0.02% NaN3 at 37 °C for 24 h and visualized by staining with Coomassie Blue R-250.

2.14. Statistical analysis

Expression data of MMPs, UA, and VEGF release were performed on triplicate samples with duplicate readings. Statistical analysis was performed using GraphPad Prism 4.02 (GraphPad Software Inc., La Jolla, CA). T-tests were performed to determine significance using GraphPad Prism 4.02. Significance levels were determined using post-tests, and were set at *$p<0.05$, **$p<0.01$, and ***$p<0.001$. All graphical data were reported.

3. Results and discussion

3.1. Control over in vitro vasculogenesis and ex ovo angiogenesis

In our previous study, we demonstrated that ECFCs undergo vascular morphogenesis within a well-defined synthetic matrix, namely AHA hydrogels modified with RGD and containing MMP-cleavable crosslinks [28]. Here, we hypothesized that cell-mediated degradation could be exploited to spatially control vascular morphogenesis during vasculogenesis of ECFCs and angiogenesis by ECFCs and *ex ovo* CAM. Two crosslinking methods were applied sequentially to form the HA hydrogels. In the primary crosslinking method, HA hydrogels are formed from AHA precursors modified with integrin-binding adhesive peptides (via conjugate addition reactions between the thiol groups on RGDS-containing peptides and acrylates along the HA backbone), and then crosslinked with dithiol peptides (thiol groups on each end of the peptide react with the acrylates) via a primary addition reaction generating uniform “−UV” hydrogels (Figure 1A). Importantly, only a fraction of the total acrylates is consumed during this first step, leaving a network that is “permissive” to proteolytic degradation. In the presence of a photoinitiator, the remaining acrylates on the HA macromer could be further crosslinked using a secondary radical reaction [30]. In this secondary step, the hydrogels are exposed to UV light, which initiates radical polymerization of the remaining acrylates, resulting in the formation of non-degradable kinetic chains, which are “inhibitory” to cell-mediated degradation (Figure 1A). This technique has been previously used to spatially control the spreading [29] and differentiation [30] of hMSCs.

We first examined if we could inhibit *in vitro* vasculogenesis of ECFCs. When encapsulated in −UV hydrogels, ECFCs were able to undergo vasculogenesis; however, within +UV hydrogels, ECFCs were able to form vacuoles and lumen, but were unable to branch and sprout, arresting the vascular morphogenesis (Figure 1B). We next examined vessel infiltration into +UV and −UV AHA hydrogels using *ex ovo* CAM. We grafted uniform −UV and +UV hydrogels onto CAM at EDD 8, at which the mitotic index of EC is optimal (Figure 2A) [41]. At EDD 12, we observed extensive vessel invasion into the “permissive” −UV hydrogels, but not into the “inhibitory” +UV hydrogels (Figure 2B and C). Histological analysis of the harvested hydrogels constructs further confirmed these observations. The “permissive” −UV hydrogels degraded and were penetrated by the CAM vessels (Figure 2D, i), while the “inhibitory” +UV hydrogels remain intact with limited vessel ingrowth (Figure 2D, ii). These two observations showed how cell-mediated

degradation can be exploited to provide spatial control over vasculogenesis and angiogenesis assays.

3.2. Differential degradation of the −UV and + UV AHA hydrogels

To better understand the mechanism by which HA hydrogels alter cellular remodeling in both of the vasculogenesis and angiogenesis assays, we characterized the physical properties of −UV and +UV hydrogels. We found that there is no significant difference in the VEGF release profile of −UV and +UV hydrogels. Both types of hydrogels released half of the encapsulated VEGF in the first day and retained 20% of the encapsulated VEGF up to day 3 (Figure 3A). These observations are in agreement with our previous report that the VEGF release profile is not affected by the hydrogel crosslinking density [32]. However, there is a significant difference in the degradation kinetics of the −UV and +UV hydrogels. The −UV hydrogels released significantly more uronic acid (UA), the byproduct of HA degradation, compared to the +UV hydrogels (Figure 3B). These results suggested that the ability of the −UV hydrogels to “permit” cellular remodeling and the ability of the +UV hydrogels to “inhibit” cellular remodeling in both vasculogenesis and angiogenesis, is attributed to the difference in their degradation kinetics, rather than their release capabilities. Moreover, elastic modulus measurements showed that UV photocrosslinking increases the elastic modulus of HA hydrogels from ~200 Pa for −UV hydrogels to ~800 Pa for +UV hydrogels (Figure 3C). This observation is in agreement with our previous study, which reports that UV crosslinking increases the elastic modulus of HA hydrogels [30]. We also observed that +UV hydrogels maintain a constant swelling ratio of 100%, while −UV hydrogels show a steady increase in swelling ratio up to 250% by day 1, at which point they reach a state of swelling equilibrium (Figure 3D). The secondary radical crosslinking created a non-degradable kinetic chain, which also resulted in a higher elastic modulus and a lower swelling rate of the +UV hydrogels compared to the −UV hydrogels.

3.3. Differential MMP expression in −UV and + UV AHA hydrogels

We further characterized the dynamic interactions between ECFCs and the two types of HA hydrogels. We analyzed MMP expression from ECFCs encapsulated in −UV and +UV hydrogels over 3 days of culture. We found that during the early culture period up to day 2, ECFCs cultured in +UV hydrogels express significantly higher levels of MMP-1, -2, and -14 compared to the ECFCs cultured in −UV hydrogels. In contrast to the MMP expression in −UV hydrogels, which increases with culture, the MMP expression in +UV hydrogels initially increases up to day 2 then decreases on day 3 (Figure 4). Zymography analysis also detected higher levels of activated MMP-1 and -2 in the conditioned media of ECFCs cultured in +UV hydrogels compared to those in −UV hydrogels (Figure 4A–B). These findings are similar to our previous study demonstrating that ECFCs cultured on stiffer matrices express higher levels of MMPs to facilitate matrix degradation and remodeling [31]. However, these high levels of MMP expression in +UV hydrogels did not result in matrix degradation due to the non-degradable bonds created by the kinetic chains (Figure 3B **above**). Moreover, MMP expression of ECFCs encapsulated in +UV hydrogels decreases at day 3 after their highest levels at day 2, suggesting the adaptability of ECFCs to their microenvironment. In response to the stiffer and non-degradable matrix, ECFCs secreted high level of MMPs to degrade their surrounding [28, 31]. Nonetheless, faced with the non-degradable kinetic chains within the +UV hydrogels, these high levels of MMP expression did not result in matrix degradation, which led to ECFC adaptation to their surroundings by decreasing the MMP expression at day 3. These results clarified our observations that ECFCs cultured within +UV hydrogels form vacuole and lumen, but are unable to branch and sprout (Figure 1B **above**), two cellular events that are tightly regulated by MMPs [23, 24]. Consequently, vascular tube and vessel infiltration were only “permitted” within the

−UV hydrogels through matrix degradation, yet were “inhibited” within the radically-crosslinked +UV hydrogels.

3.4. Spatial control of ECFC remodeling for in vitro vasculogenesis

A photomask was used to exploit the sequential crosslinking system, to generate −UV and +UV regions within the hydrogels. In the +UV region, the remaining free acrylate groups are further crosslinked, creating networks “inhibitory” to cell-mediated degradation and spreading (Figure 5A) [29]. A variety of photomasks can be used to generate hydrogels with different sizes and patterns of −UV and +UV regions (Figure 5B). Within the −UV regions, we observed that ECFCs are able to form vacuole and lumen, branches and sprouts, and form vascular tube networks as was previously reported (Figure 5B) [28]. The +UV regions are labeled with MeRho, as it reacted rapidly with the free acrylate groups under UV exposure [29, 30], and are bordered with dotted white lines. Within +UV regions, ECFCs were able to form vacuoles and lumen, but were unable to branch and sprout, arresting the vascular morphogenesis at this stage (Figure 5C). We observed that the −UV regions are “permissive” to the complete stages of vascular morphogenesis. ECFCs encapsulated within the “permissive” −UV regions are able to form vacuoles and lumen, branch and sprout, and eventually form vascular networks. In contrast, the +UV regions are “inhibitory” to the stages of branching and sprouting, which are considered as MMP-dependent mechanisms. Due to the existence of kinetic chains within the “inhibitory” +UV region, ECFCs can form vacuole and lumen, but are not able to branch and sprout in order to form vascular networks (Figure 6). Hence, this photopatterning technique can be used to spatially control vascular tube formation of ECFCs during vasculogenesis in hydrogels. The ability to spatially control vascular networks within synthetic biomaterials can benefit the generation of more complex and organized vasculatures, which in turn can improve the survival and functionality of tissue-engineered organs [14].

3.5. Spatial control over in vitro angiogenesis

To mimic the process of angiogenesis, Davis and colleagues developed an *in vitro* angiogenesis assay using collagen gels [5, 34]. In response to SDF-1α and S1P, a confluent monolayer of endothelial cells (ECs) are shown to invade and sprout into the collagen gels underneath in a way that mimics the appearance of tip cells from pre-existing blood vessels [34]. Here, we hypothesized that HA hydrogels could be used as an *in vitro* angiogenesis assay, and as such, provide opportunities to elucidate the role of matrix remodeling during angiogenesis in synthetic biomaterials. After 3 days in culture, a confluent monolayer of ECFCs invaded and sprouted into the 3D hydrogels (Figure 7A). Since ECFCs invasion and sprouting requires matrix degradation, which mainly relies on MMP activities [31], we further examined whether photopatterned hydrogels could be used to direct angiogenesis by ECFCs. Using a 100 μm-wide stripe pattern, ECFCs invasion and sprouting was permitted within −UV regions and inhibited within the +UV region (Figure 7B). Confluent monolayers of ECFCs began to sprout and invade into the −UV region (Figure 7Bi), and further branched along the −UV region (Figure 7Bii). ECFCs were not able to invade and sprout into the +UV region due to the non-degradable kinetic chains formed by the secondary radical crosslinking. Thus, this photopatterning technique based on cell-mediated degradation can be further used to direct ECFCs during angiogenic invasion and sprouting.

4. Conclusions

Collectively, we have shown how synthetic and tunable HA hydrogels can be used as vasculogenesis and angiogenesis assays, which provide unique opportunities to elucidate the role of matrix remodeling throughout these processes. Furthermore, we demonstrated how manipulating the degradability of synthetic biomaterials can be used to provide spatial

degradation cues, which are either “permissive” or “inhibitory” to vascular tube formation. With high spatial precision, we can create −UV regions, which are “permissive” to vascular tube formation and +UV regions, which are “inhibitory” to vascular tube formation. Our understanding and ability to control degradation cues that “permit” or “inhibit” vasculogenesis and angiogenesis in synthetic biomaterials can be valuable for the basic study of vascular biology and for the application of improving vascular organization in tissue engineering.

Acknowledgments

We thank Dr. Beatrice Kondo and Jane Yee from JHU for assisting with the CAM assay; and Drs. Jennifer Elisseeff and Jeannine Coburn from JHU for assisting with microrheology measurements. This research was partially funded by an NSF graduate research fellowship (to SK), an AHA-Scientist Development grant and NIH grant R01HL107938 (both to SG) and NIH grant U54CA143868.

References

1. Carmeliet P. Mechanisms of angiogenesis and arteriogenesis. Nat Med. 2000; 6(4):389–95. [PubMed: 10742145]
2. Jain RK. Molecular regulation of vessel maturation. Nat Med. 2003; 9(6):685–93. [PubMed: 12778167]
3. Richardson MR, Yoder MC. Endothelial progenitor cells: Quo Vadis? J Mol Cell Cardiol. 2011; 50(2):266–72. [PubMed: 20673769]
4. Iruela-Arispe ML, Davis GE. Cellular and Molecular Mechanisms of Vascular Lumen Formation. Dev Cell. 2009; 16(2):222–31. [PubMed: 19217424]
5. Davis GE, Kon W, Stratman AN. Mechanisms controlling human endothelial lumen formation and tube assembly in three-dimensional extracellular matrices. Birth Defects Res C Embryo Today. 2007; 81(4):270–85. [PubMed: 18228260]
6. Kniazeva E, Putnam AJ. Endothelial cell traction and ECM density influence both capillary morphogenesis and maintenance in 3-D. Am J Physiol Cell Physiol. 2009; 297(1):C179–C187. [PubMed: 19439531]
7. Bayless KJ, Salazar R, Davis GE. RGD-Dependent Vacuolation and Lumen Formation Observed during Endothelial Cell Morphogenesis in Three-Dimensional Fibrin Matrices Involves the alpha(v)beta(3) and alpha(5)beta(1) Integrins. Am J Pathol. 2000; 156(5):1673–83. [PubMed: 10793078]
8. Shamloo A, Heilshorn SC. Matrix density mediates polarization and lumen formation of endothelial sprouts in VEGF gradients. Lab Chip. 2010; 10(22):3061–8. [PubMed: 20820484]
9. Senger D, Galli S, Dvorak A, Perruzzi C, Harvey V, Dvorak H. Tumor cells secrete a vascular permeability factor that promotes accumulation of ascites fluid. Science. 1983; 219(4587):983–5. [PubMed: 6823562]
10. Folkman J, Klagsbrun M. Angiogenic factors. Science. 1987; 235(4787):442–7. [PubMed: 2432664]
11. Folkman J. Angiogenesis: an organizing principle for drug discovery? Nat Rev Drug Discov. 2007; 6(4):273–86. [PubMed: 17396134]
12. Davis GE, Senger DR. Extracellular matrix mediates a molecular balance between vascular morphogenesis and regression. Curr Opin Hematol. 2008; 15(3):197–203. [PubMed: 18391785]
13. Davis GE, Senger DR. Endothelial extracellular matrix: biosynthesis, remodelling, and functions during vascular morphogenesis and neovessel stabilization. Circ Res. 2005; 97(11):1093–107. [PubMed: 16306453]
14. Koffler J, Kaufman-Francis K, Shandalov Y, Egozi D, Amiad Pavlov D, Landesberg A, et al. Improved vascular organization enhances functional integration of engineered skeletal muscle grafts. Proc Natl Acad Sci U S A. 2011; 108(36):14789–94. [PubMed: 21878567]
15. Dickinson LE, Moura ME, Gerecht S. Guiding endothelial progenitor cell tube formation using patterned fibronectin surfaces. Soft Matter. 2010; 6:5109–19.

16. Hanjaya-Putra DG, Sharon. Mending the Failing Heart with a Vascularized Cardiac Patch. Cell Stem Cell. 2009; 5(6):575–6. [PubMed: 19951684]
17. Phelps EA, Landázuri N, Thulé PM, Taylor WR, García AJ. Bioartificial matrices for therapeutic vascularization. Proc Natl Acad Sci U S A. 2010; 107(8):3323–8. [PubMed: 20080569]
18. Zisch AH, Lutolf MP, Ehrbar M, Raeber GP, Rizzi SC, Davies N, et al. Cell-demanded release of VEGF from synthetic, biointeractive cell ingrowth matrices for vascularized tissue growth. FASEB J. 2003; 17(15):2260–2. [PubMed: 14563693]
19. Moon JJ, Saik JE, Poché RA, Leslie-Barbick JE, Lee S-H, Smith AA, et al. Biomimetic hydrogels with pro-angiogenic properties. Biomaterials. 2010; 31(14):3840–7. [PubMed: 20185173]
20. Chen, YC.; Lin, RZ.; Qi, H.; Yang, Y.; Bae, H.; Melero-Martin, JM., et al. Functional Human Vascular Network Generated in Photocrosslinkable Gelatin Methacrylate Hydrogels. Adv Funct Mater. 2012. Available from URL: http://onlinelibrary.wiley.com/doi/10.1002/adfm.201101662/abstract
21. Lutolf MP, Hubbell JA. Synthetic biomaterials as instructive extracellular microenvironments for morphogenesis in tissue engineering. Nat Biotech. 2005; 23(1):47–55.
22. Culver JC, Hoffmann JC, Poché RA, Slater JH, West JL, Dickinson ME. Three-Dimensional Biomimetic Patterning in Hydrogels to Guide Cellular Organization. Adv Mater. 2012; 24(17): 2344–8. [PubMed: 22467256]
23. Stratman AN, Saunders WB, Sacharidou A, Koh W, Fisher KE, Zawieja DC, et al. Endothelial cell lumen and vascular guidance tunnel formation requires MT1-MMP-dependent proteolysis in 3-dimensional collagen matrices. Blood. 2009; 114(2):237–47. [PubMed: 19339693]
24. Chun TH, Sabeh F, Ota I, Murphy H, McDonagh KT, Holmbeck K, et al. MT1-MMP-dependent neovessel formation within the confines of the three-dimensional extracellular matrix. J Cell Biol. 2004; 167(4):757–67. [PubMed: 15545316]
25. Chwalek K, Levental KR, Tsurkan MV, Zieris A, Freudenberg U, Werner C. Two-tier hydrogel degradation to boost endothelial cell morphogenesis. Biomaterials. 2011; 32(36):9649–57. [PubMed: 21937106]
26. Toole BP. Hyaluronan: from extracellular glue to pericellular cue. Nat Rev Cancer. 2004; 4(7): 528–39. [PubMed: 15229478]
27. Gerecht S, Burdick JA, Ferreira LS, Townsend SA, Langer R, Vunjak-Novakovic G. Hyaluronic acid hydrogel for controlled self-renewal and differentiation of human embryonic stem cells. Proc Natl Acad Sci U S A. 2007; 104(27):11298–303. [PubMed: 17581871]
28. Hanjaya-Putra D, Bose V, Shen Y-I, Yee J, Khetan S, Fox-Talbot K, et al. Controlled activation of morphogenesis to generate a functional human microvasculature in a synthetic matrix. Blood. 2011; 118(3):804–15. [PubMed: 21527523]
29. Khetan S, Katz JS, Burdick JA. Sequential crosslinking to control cellular spreading in 3-dimensional hydrogels. Soft Matter. 2009; 5:1601–6.
30. Khetan S, Burdick JA. Patterning network structure to spatially control cellular remodeling and stem cell fate within 3-dimensional hydrogels. Biomaterials. 2010; 31(32):8228. [PubMed: 20674004]
31. Hanjaya-Putra D, Yee J, Ceci D, Truitt R, Yee D, Gerecht S. Vascular endothelial growth factor and substrate mechanics regulate in vitro tubulogenesis of endothelial progenitor cells. J Cell Mol Med. 14(10):2436–47. [PubMed: 19968735]
32. Yee D, Hanjaya-Putra D, Bose V, Luong E, Gerecht S. Hyaluronic Acid Hydrogels Support Cord-Like Structures from Endothelial Colony-Forming Cells. Tissue Eng Part A. 2011; 17(9–10): 1351–61. [PubMed: 21247340]
33. Yoder MC, Mead LE, Prater D, Krier TR, Mroueh KN, Li F, et al. Redefining endothelial progenitor cells via clonal analysis and hematopoietic stem/progenitor cell principals. Blood. 2007; 109(5):1801–9. [PubMed: 17053059]
34. Bayless KJ, Kwak H-I, Su S-C. Investigating endothelial invasion and sprouting behavior in three-dimensional collagen matrices. Nat Protoc. 2009; 4(12):1888–98. [PubMed: 20010936]
35. Auerbach R, Kubai L, Knighton D, Folkman J. A simple procedure for the long term cultivation of chicken embryos. Dev Biol. 1974; 41(2):391–4. [PubMed: 4452416]

36. Mammoto A, Connor KM, Mammoto T, Yung CW, Huh D, Aderman CM, et al. A mechanosensitive transcriptional mechanism that controls angiogenesis. Nature. 2009; 457(7233): 1103–8. [PubMed: 19242469]

37. Janssen L, Vanderhooft MA, Magda Jules J, Prestwich Glenn D. Rheological Properties of Cross-Linked Hyaluronan-Gelatin Hydrogels for Tissue Engineering. Macromol Biosci. 2009; 9(1):20–8. [PubMed: 18839402]

38. Sun G, Shen Y-I, Kusuma S, Fox-Talbot K, Steenbergen CJ, Gerecht S. Functional neovascularization of biodegradable dextran hydrogels with multiple angiogenic growth factors. Biomaterials. 2011; 32(1):95–106. [PubMed: 20870284]

39. Sun G, Shen YI, Ho CC, Kusuma S, Gerecht S. Functional groups affect physical and biological properties of dextran-based hydrogels. J Biomed Mater Res A. 2010; 93(3):1080–90. [PubMed: 19753626]

40. Raeber GP, Lutolf MP, Hubbell JA. Molecularly engineered PEG hydrogels: A novel model system for proteolytically mediated cell migration. Biophys J. 2005; 89(2):1374–88. [PubMed: 15923238]

41. Ribatti D, Vacca A, Roncali L, Dammacco F. The chick embryo chorioallantoic membrane as a model for in vivo research on angiogenesis. Int J Dev Biol. 1996; 40(6):1189–97. [PubMed: 9032025]

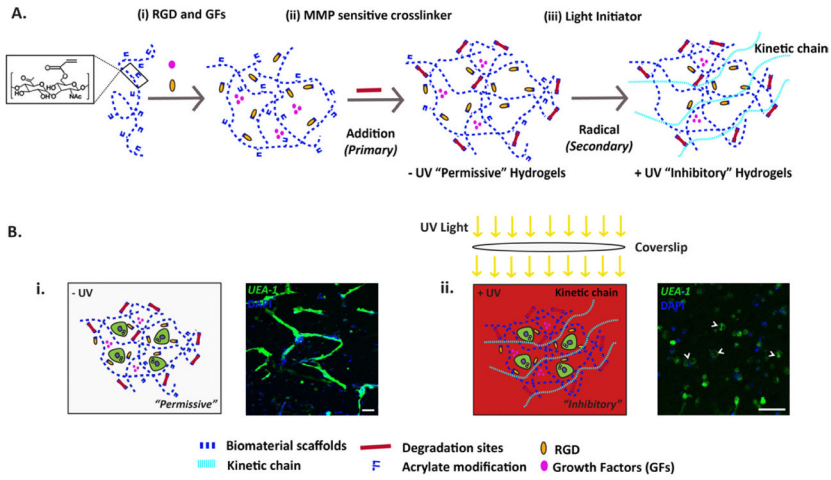

Figure 1. AHA Hydrogel Schematic

(**A**) Schematic of AHA hydrogel formation with sequential crosslinking. (i) Soluble growth factors (GFs) are mixed with AHA and RGD-containing peptides. (ii) The hydrogels are then crosslinked by the addition of MMP-sensitive crosslinkers using a primary addition reaction to create a "permissive" −UV hydrogels. (iii) The free acrylate groups can be further crosslinked in the presence of photoinitiator and UV light using a secondary radical reaction to create "inhibitory" +UV hydrogels. (**B**) Differential effect of hydrogels degradability on vasculogenesis. (i) Within the −UV hydrogels, encapsulated ECFCs undergo complete vasculogenesis to form complex vascular tube networks. (ii) Within the +UV hydrogels, where kinetic chains are generated through the secondary radical crosslinking, encapsulated ECFCs only form vacuole and lumen (***arrowhead***), but failed to branch and sprout. ECFCs are stained with Fluorescein-conjugated *UEA-I* lectin (***green***) and DAPI (***blue***). Scale bars are 100 μm.

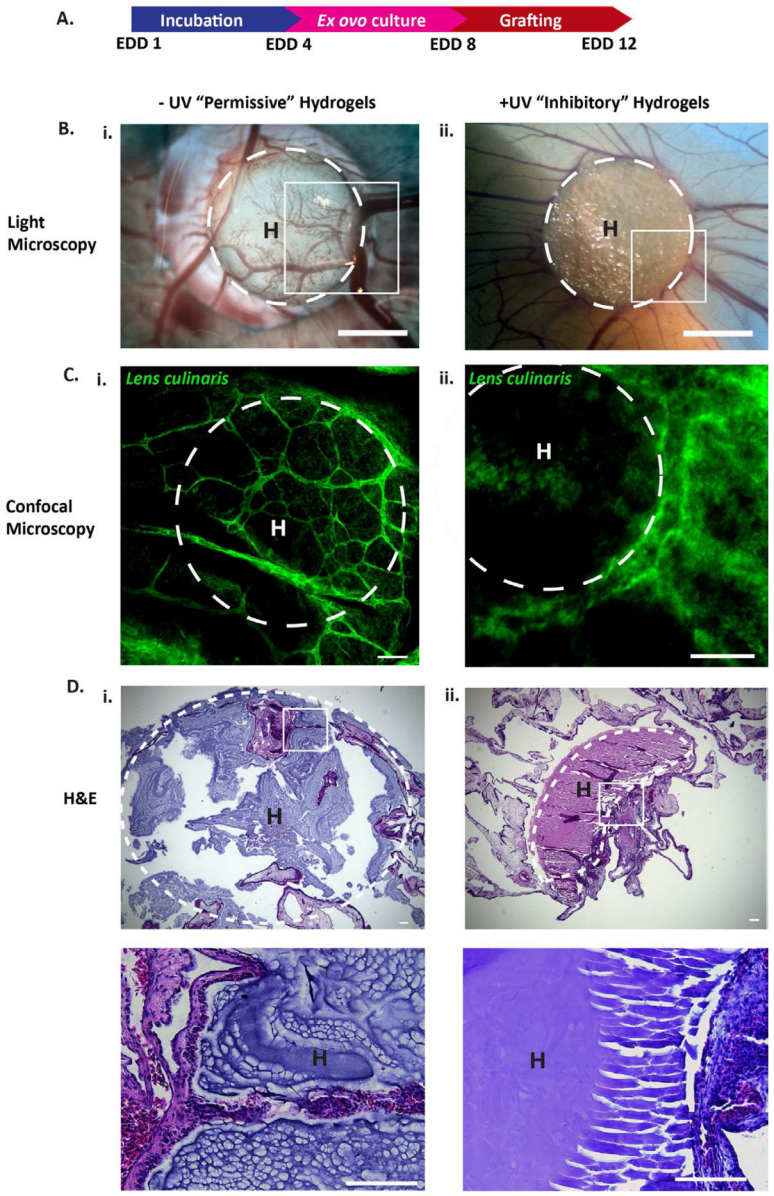

Figure 2. Control over *ex ovo* angiogenesis

(**A**) Uniform −UV and +UV AHA hydrogels are grafted onto the CAM membrane at EDD 8 and harvested at EDD 12. (**B**) LM imaging and (**C**) confocal analysis of the boxed regions in **B** shows CAM vessels penetrating into the −UV but not into the +UV hydrogels. CAM vessels are stained with Fluorescein-conjugated *Lens culinaris* lectin. (**D**) H&E analysis further shows that −UV hydrogels are degraded (***i***, and ***inset***), while the +UV hydrogels remain intact (***ii***, and ***inset***). Scale bars in: **B** is 20 mm, **C–D** are 100 μm. **H** = hydrogels. Dotted white lines indicate the boundaries of the hydrogels.

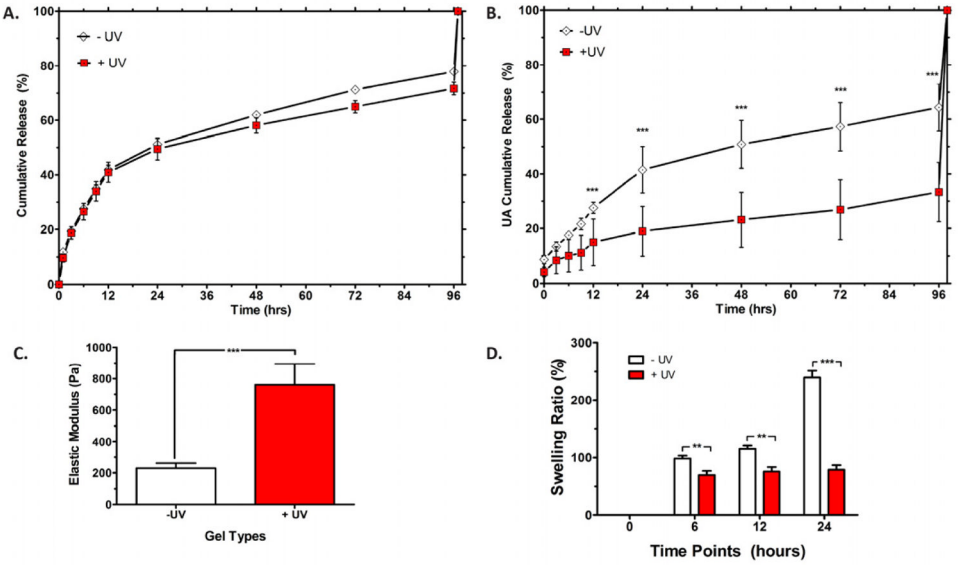

Figure 3. Physical properties of the − UV and +UV Hydrogels

(A) VEGF release profiles from −UV and +UV hydrogels over 3 days are reported as cumulative release. (**B**) Degradation kinetics of uniform −UV and +UV hydrogels as detected by the cumulative release of uronic acid (UA). (**C**) Elastic modulus of uniform −UV and +UV hydrogels as measured using microrheology. (**D**) Swelling ratio of uniform −UV and +UV hydrogels. Significance levels are set at **p<0.01 and ***p<0.001.

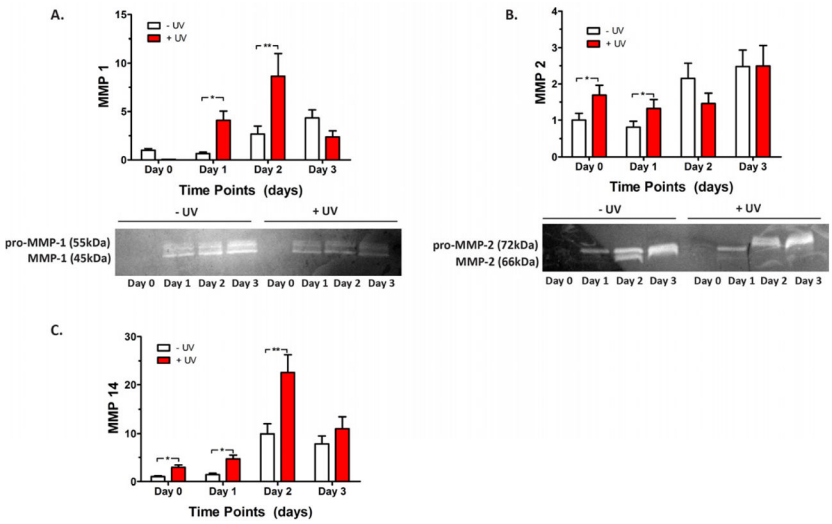

Figure 4. Differential MMP Expression in −UV and +UV hydrogels

Encapsulated ECFCs in −UV and +UV hydrogels are evaluated for their MMP expression using real time RT-PCR including MMP-1 (**A**), MMP-2 (**B**), and MMP-14 (**C**). Zymography analysis also reveals higher levels of activated MMP-1 (**A, *bottom***) and MMP-2 (**B, *bottom***) in the culture media of ECFCs grown in +UV hydrogels than −UV hydrogels. Significance levels are set at *p<0.05 and **p<0.01.

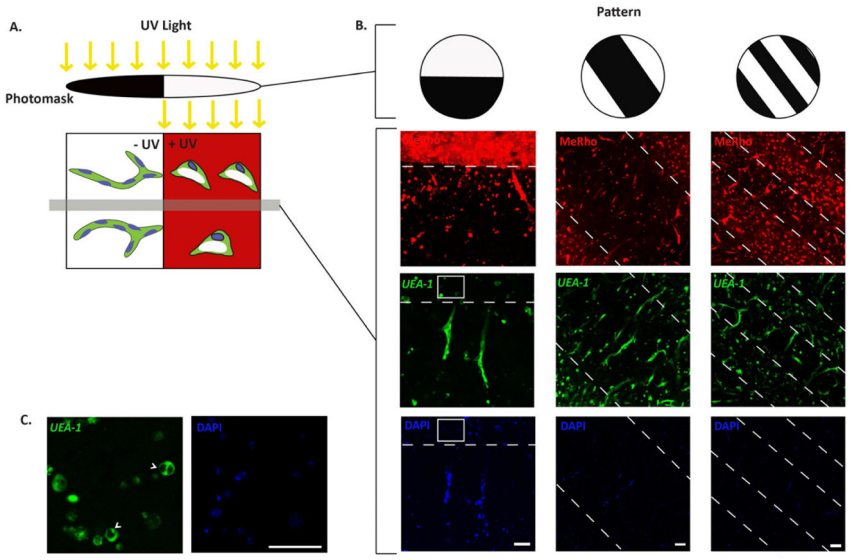

Figure 5. Spatial control over *in vitro* vasculogenesis

(**A**) Schematic diagram of photopatterning of AHA hydrogels using UV light and photomasks to create −UV and +UV regions. (**B**) Representative confocal images of photopatterned AHA hydrogels with various patterns. Vascular tube formation is detected within the −UV regions but not within the +UV regions (labeled using MeRho (***red***) and bordered with dotted white lines). (**C**) Only vacuole and lumen formation (***arrowhead***) are found in ECFCs encapsulated within the +UV regions; high magnification inset of the boxed area in (**B**). ECFCs are stained with Fluorescein-conjugated *UEA-I* lectin (***green***) and DAPI (***blue***). Scale bars are 100 μm.

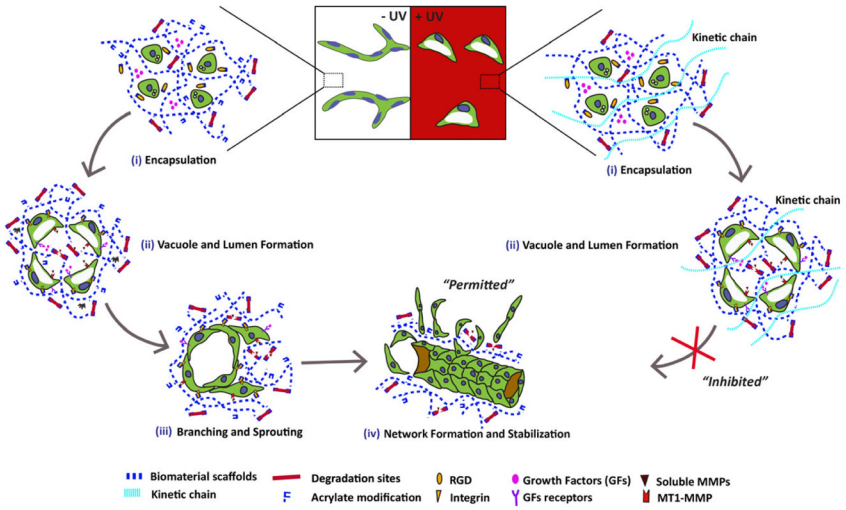

Figure 6. HA Hydrogels for Spatially Controlled Vascular Morphogenesis

Within the −UV region, vascuologenesis is "permitted." Encapsulated ECFCs cultured within the −UV region are able to form vacuoles and lumens, followed by branching and sprouting, and eventually form complex vascular networks. Photocrosslinking introduces non–degradable kinetic chains within the +UV region, thus inhibiting branching, sprouting, and the formation of complex vascular networks.

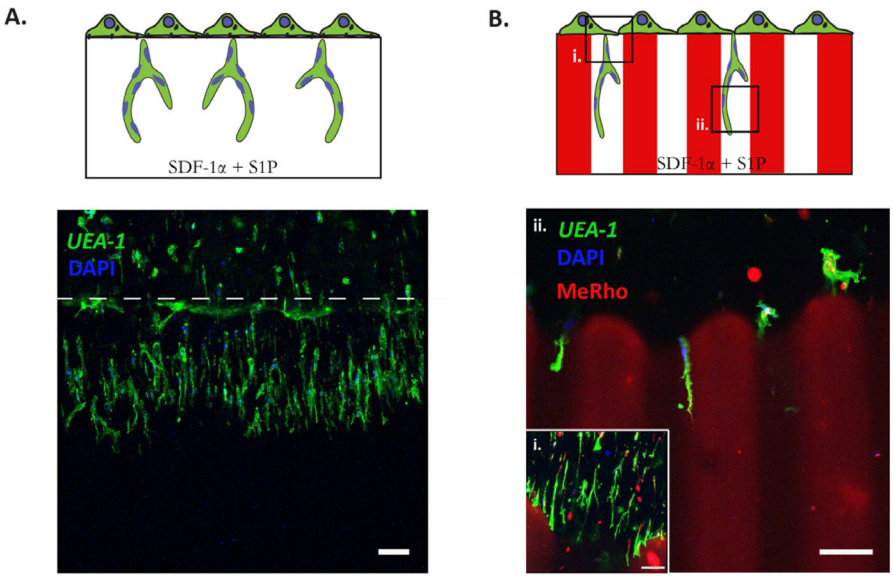

Figure 7. Spatial control over *in vitro* angiogenesis

ECFCs are seeded on top of a uniform −UV (**A**) and 100 μm stripe photopatterned (**B**) HA hydrogels for angiogenesis assay. After 3 days in culture, ECFCs invade and sprout into the 3D hydrogels (**A**) When photopatterned HA hydrogels are used, invasion and sprouting are observed only within the −UV regions and not within the inhibitory +UV region (**B**). Confluent monolayer of ECFCs sprouts and invades the −UV region (**i**), and further branches along the −UV regions (**ii**). The +UV regions are labeled using MeRho (***red***), ECFCs are stained with Fluorescein-conjugated *UEA-I* lectin (***green***) and DAPI (***blue***). Scale bars are 100 μm.